A. MANJUNATH[1*], V. ANANDAKRISHNAN[2], S. RAMACHANDRA[1], K. PARTHIBAN[1], S. SATHISH[3]

# OPTIMIZATION OF TRIBOLOGICAL PARAMETERS OF PRE-POSITIONED WIRE BASED ELECTRON BEAM ADDITIVE MANUFACTURED TI-6AL-4V ALLOY

The versatile application of titanium alloy in the aerospace industry and it's hard to machine characteristics focus towards the additive manufacturing. The Ti-6Al-4V alloy is manufactured using the electron beam source with a novel method of prepositioned titanium alloy wires. The tribology of the additive manufactured titanium alloy under dry sliding condition is experimented and analysed using Taguchi technique. The targeted objective of minimum tribological responses are attained with the identified optimal parameters as load – 9.81 N, sliding velocity – 3 m/s, sliding distance – 3000 m for minimum specific wear rate and load – 9.81 N, sliding velocity – 3 m/s, sliding distance – 1000 m for minimum coefficient of friction. Among the parameters tested, load is found to be the dominant factor on the tribology of additively manufactured titanium alloy. The morphological analysis on the worn surface and debris revealed the existence of abrasion, delamination and adhesion wear mechanisms. The increase in the load dominantly showed the appearance of delamination mechanism.

*Keywords:* Additive manufacturing; dry sliding wear; titanium alloy; wear analysis; wear mechanisms

## Nomenclature

DF — degrees of freedom
Seq SS — sequential sums of squares
Adj SS — adjusted sums of squares
Adj MS — adjusted mean squares
P — probability
C% — contribution percentage

## 1. Introduction

Material with lower density, higher strength and good properties at elevated temperatures is highly needed in the aerospace and defence industries. Titanium alloy is the one which is best suited to the requirements mentioned above [1-3]. Ti-6Al-4V is the most used material in the available titanium alloys with higher resistance to thermal and corrosion [4]. The major problem experienced while handling Ti-6Al-4V is it's hard to machine as it is very hard [5]. Notably, the attainment of the complex geometry of gas turbine blades with Ti-6Al-4V alloy is more complicated. The reduction in the process of machining can be achieved with the production of components to its near-net shape, and this can be achieved with additive manufacturing. Also, it is well known that the material property highly relies on the selection of processing routes (i.e., if a material is process through casting it will have some properties and if the same is processed through powder metallurgy it will differ). In a similar way there is no proscription with the materials processed through additive manufacturing too. As per the terminology of joint ASTM/ISO, Additive manufacturing is the process of joining materials to make the parts from the 3D data model with the concept of layer by layer generation [6]. Wire based additive manufacturing technology is employed for the present research, where the titanium alloy wire is melted and then solidified to attain the required geometry of parts with the help of high energy electron beam source. The process involves in the solidification of material at higher rate which eventually end up in variations of thermal gradient. The most important factor such as temperature gradient, solidification rate undercooling of liquid phase and alloy constitution has a significant effect on the microstructure of additive manufactured material. This will results in changes in microstructure that lead to varied mechanical properties and induced residual stresses. The stress distribution differs with the part geometry. Particularly, when working with alloys it does not have a specific melting instead it has a solidification range that causes the alloy elements

1 GAS TURBINE RESEARCH ESTABLISHMENT, DEFENCE RESEARCH & DEVELOPMENT ORGANIZATION, BANGALORE, KARNATAKA-560093, INDIA
2 DEPARTMENT OF PRODUCTION ENGINEERING, NATIONAL INSTITUTE OF TECHNOLOGY TIRUCHIRAPALLI, TIRUCHIRAPPALLI – 620015, TAMIL NADU, INDIA
3 DEPARTMENT OF MECHATRONICS ENGINEERING, K. S. RANGASAMY COLLEGE OF TECHNOLOGY, TIRUCHENGODE, NAMAKKAL – 637215, TAMIL NADU, INDIA

* Corresponding author: manjunathgtre@gmail.com

to redistribute between solid and liquid. Ti64 alloy is the most important material comes under the columnar microstructure which has less than 10 K solidification range [7-9]. The observation of microstructural variation is reported in the titanium alloy with different techniques of addtive manufacturing processes i.e., transformation of α' martensite from vertical β grain during quenching in selective laser melting and lamellar α + β in wire electron beam machining [10]. In general, the rapid solidification results in fine microstructural features, including fine grains, or closely-spaced dendrites. The above alteration in the microstructure supports in the property variations. The wire prepositioned additive manufacturing can overcome the significant drawback of higher production cost. Using the prepositioned additive manufacturing technique, the Ti-6Al-4V titanium alloy was manufactured at different parameters, and its effect on the bead geometry is analysed [11]. Likewise, the research focus on the wire additive manufacturing of metallic components using an electron beam source showed successful accomplishments [12-15]. The metallurgical and mechanical properties of such additive manufactured titanium alloys are established. The performance of the material in view of tribology is needed to explore. Some of the earlier research works on the tribology of titanium alloys are as follows. The wear perfromance behaviour of titanium alloy (Ti-6Al-4V) is examined in the lubricated sliding condition, which shows a positive effect on the wear behaviour with increased sliding velocity [16]. The wear perfromance of titanium alloy (Ti-6Al-4V) is examined under a dry condition with varied parameters, which shows a positive effect on the wear behaviour with increased load and sliding velocity [17]. The wear perfromance of titanium alloy (Ti-6Al-4V) is examined in the dry sliding state, which shows the wear mechanism transition condition in respect of sliding velocity [18]. The wear perfromance of rolled titanium alloy (Ti-6Al-4V) is examined in the dry sliding state in varied parameters, which shows the dominance of delamination and oxidation mechanisms [19]. The wear behaviour of titanium alloy processed through selective laser melting is examined in the dry under lubricated condition, which shows the presence of oxidation, delamination and abrasion mechanisms [20]. The literature shows the influence of processess in the variaions of microstructure and the necessity of the exploration of performance of material property. Hence, the present work aims on the exploration of tribological performance of wire additive manufactured titanium alloy with the help of taguchi analysis. In addition, the morphological analysis on the worn surface and debris is conducted to explore the responsible wear mechanisms.

## 2. Methodology

### 2.1. Material synthesis

The work material Ti-6Al-4V alloy was synthesized by the fusion of prepositioned titanium 64 alloy filler wire using the electron beam source. The pilot experiments were carried out with varied electron beam welding parameters. The additive sample made with the accelerating voltage of 140 kV, welding speed of 600 mm/min and beam current of 8 mA shows complete fusion and is free from defects. With the identified suitable parameter combination, the additive samples were made in the form of a plate of 100×7.8×7.5 mm with the successive fusion of prepositioned titanium 64 alloy filler wires. From the additive manufactured plate, test samples for metallographic analysis were segmented and analysed. Also, the test sample for wear experimentation is extracted from the additive manufactured plate in the form of pins 6 mm diameter with 25 mm length. The x-ray diffraction analysis and the scanning electron microscopic analysis was performed in Rigaku Ultima diffractometer (2theta range: 0 to 90°) and Vega 3 Tescan microscope, respectively.

### 2.2. Wear experiments

The wire additive manufactured wear samples, and the counterpart disc was polished to obtain the surface roughness of less than 0.8 microns. Following the ASTM G99 standard, the wear experimentations were experimented out in the Pin-on-disc experiment in dry situation with the counterpart as hardened D3 steel. The combination of experiments in consideration with the parameters load, sliding velocity and sliding distance are

TABLE 1

Experimental design with specific wear rate
and coefficient of friction

| Exp. No | Load, N | Sliding Velocity, m/s | Sliding Distance, m | Specific wear rate, $\times 10^{-3}$ mm$^3$/Nm | Coefficient of friction |
|---|---|---|---|---|---|
| 1 | 9.81 | 1 | 1000 | 0.1200 | 0.1805 |
| 2 | 9.81 | 1 | 2000 | 0.1412 | 0.2180 |
| 3 | 9.81 | 1 | 3000 | 0.1703 | 0.2155 |
| 4 | 9.81 | 2 | 1000 | 0.0851 | 0.0912 |
| 5 | 9.81 | 2 | 2000 | 0.0840 | 0.1131 |
| 6 | 9.81 | 2 | 3000 | 0.0823 | 0.1248 |
| 7 | 9.81 | 3 | 1000 | 0.0503 | 0.0071 |
| 8 | 9.81 | 3 | 2000 | 0.0400 | 0.0169 |
| 9 | 9.81 | 3 | 3000 | 0.0270 | 0.0446 |
| 10 | 19.62 | 1 | 1000 | 0.1537 | 0.2216 |
| 11 | 19.62 | 1 | 2000 | 0.1836 | 0.2489 |
| 12 | 19.62 | 1 | 3000 | 0.1931 | 0.2647 |
| 13 | 19.62 | 2 | 1000 | 0.1400 | 0.1835 |
| 14 | 19.62 | 2 | 2000 | 0.1535 | 0.2074 |
| 15 | 19.62 | 2 | 3000 | 0.1386 | 0.2140 |
| 16 | 19.62 | 3 | 1000 | 0.1460 | 0.1462 |
| 17 | 19.62 | 3 | 2000 | 0.1108 | 0.1598 |
| 18 | 19.62 | 3 | 3000 | 0.0704 | 0.1726 |
| 19 | 29.43 | 1 | 1000 | 0.2109 | 0.2645 |
| 20 | 29.43 | 1 | 2000 | 0.2309 | 0.2801 |
| 21 | 29.43 | 1 | 3000 | 0.2340 | 0.3098 |
| 22 | 29.43 | 2 | 1000 | 0.2201 | 0.2706 |
| 23 | 29.43 | 2 | 2000 | 0.1994 | 0.2896 |
| 24 | 29.43 | 2 | 3000 | 0.1765 | 0.2942 |
| 25 | 29.43 | 3 | 1000 | 0.2118 | 0.2582 |
| 26 | 29.43 | 3 | 2000 | 0.1795 | 0.2755 |
| 27 | 29.43 | 3 | 3000 | 0.1546 | 0.2894 |

displayed in TABLE 1 along with the specific wear rate and coefficient of friction [18,21-25]. The response specific wear rate and coefficient of friction were calculated using the standard relationship with the experimental results [26-28]. After the wear experiments, the wear debris was collected, and the worn pins were trimmed for further microscopic analysis.

# 3. Results and discussion

## 3.1. Metallurgical analysis

Figure 1 shows the x-ray diffraction analysis performed on the additive manufactured titanium alloy. The diffraction peaks resemble with the JCPDS pattern 98-009-2053. The diffraction peaks display the dominance of α phase with peak match at 35°, 38°, 40°, 53° and 70° holding the plane indices of (010), (002), (011), (012), and (013) respectively. Further, the microscopic image of the additive manufactured titanium alloy shown in Figure 2, displays the dominance of acicular α phase in the needle form. This formation of acicular α phase is due to the result of rapid cooling [29].
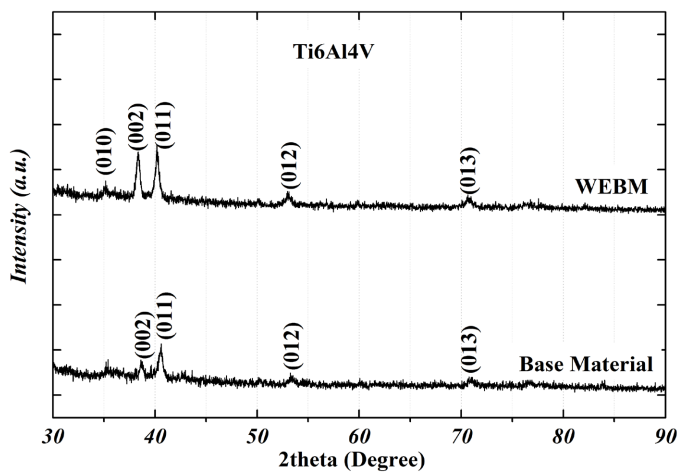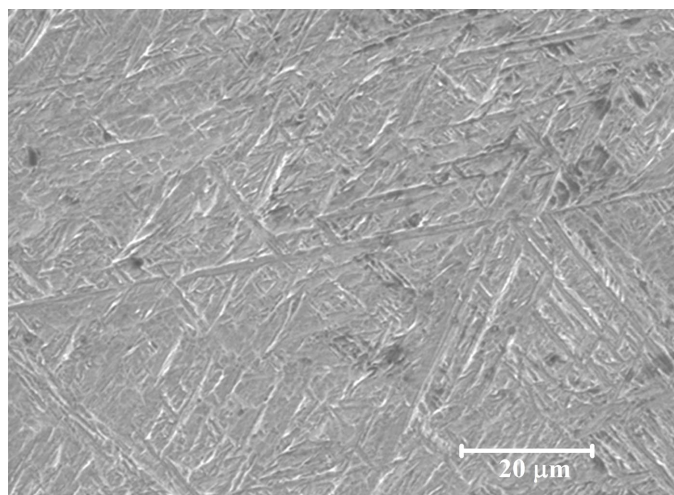


Fig. 1. X ray diffraction of additive sample



Fig. 2. Microstructure of additive manufactured titanium alloy

## 3.2. Tribological analysis

The tribological responses of specific wear rate and coefficient of friction are analyzed through Taguchi technique with the "Smaller the Better" characteristics [30]. The objective of the analysis is to identify the optimal solution and the significant parameters that contribute to the tribology of additively manufactured titanium alloy. The objective of the least specific wear rate can be obtained with the optimal solution of 9.81 N load, 3 m/s sliding velocity and 3000 m sliding distance (Figure 3a). Likewise, the objective of least coefficient of friction can be obtained with the optimal solution of 9.81 N load, 3 m/s sliding velocity and 1000 m sliding distance (Figure 3b).
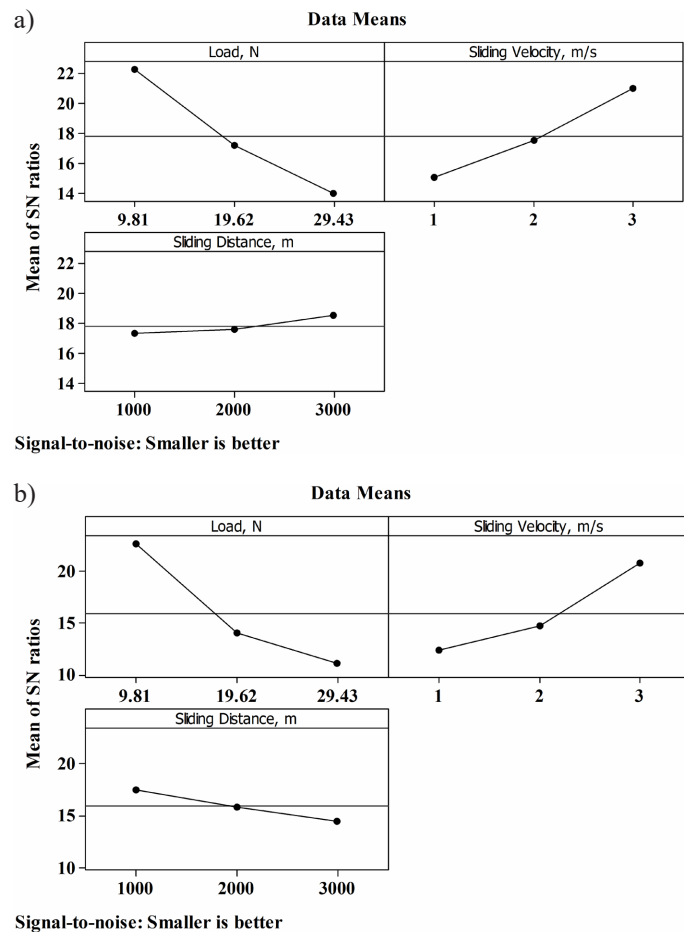


Fig. 3. Optimal plot for: (a) specific wear rate; (b) coefficient of friction

### 3.2.1. Consequence of load on specific wear rate and coefficient of friction

The influence of the parameter load over the specific wear rate is observed to be higher when compared to other parameters, namely sliding velocity and sliding distance. This has been identified with the response table, as shown in TABLE 2, which displays the higher delta value of 8.33 for load with a ranking of 1. Besides, the parameter load and the interaction of load with sliding velocity exhibits the significance of the specific wear rate in the analysis of variance (TABLE 3). The highest parameter

450

contribution of 62.43% is perceived for the load. Likewise, the analysis pertaining to the coefficient of friction displays similar observation with the dominance of load (TABLE 4). Though the analysis of variance displays significance for all the three parameters, load shows its dominance. The highest parameter contribution of 65.84% is perceived for load and 11.38% for the interaction of load with sliding velocity. As per the Archard equation, the wear rate is directly relates with applied load, and thus rise in the amount of load results in the increased wear rate. This is the reason behind the dominance of load over the specific wear rate of additively manufactured titanium alloy.

the specific wear rate with the contribution of 25.35%. Likewise, the analysis pertaining to the coefficient of friction displays alike observation with the delta value of 8.45 (TABLE 4). Though the analysis of variance displays significance for all the three parameters, sliding velocity shows its significant dominance on the coefficient of friction with the contribution of 19.76% for sliding velocity and 11.38% for the interaction of load with sliding velocity. In most cases, it is perceived that the increased sliding velocity supports on the wear resistance to a specific limit owing to the oxide formation due to the chemical reactions. Beyond that limit, it results in the reduction in wear resistance with the transition to wear mechanisms.

TABLE 2

Specific wear rate response table for SN ratio

| Level | Load, N | Sliding Velocity, m/s | Sliding distance, m |
|---|---|---|---|
| 1 | 22.30 | 14.99 | 17.33 |
| 2 | 17.18 | 17.48 | 17.58 |
| 3 | 13.97 | 20.98 | 18.54 |
| Delta | 8.33 | 5.98 | 1.20 |
| Rank | 1 | 2 | 3 |

### 3.2.3. Consequence of sliding distance on specific wear rate and coefficient of friction

The sliding distance is positioned at rank 3 for specific wear rate with least delta value of 1.20 from the response table (TABLE 2). The analysis of variance (TABLE 3) shows the non-significance to the parameter sliding distance with the probability

TABLE 3

Specific wear rate analysis of variance

| Parameters | DF[a] | Seq SS[b] | Adj SS[c] | Adj MS[d] | F | P[e] | C% |
|---|---|---|---|---|---|---|---|
| Load, N | 2 | 0.05754 | 0.05754 | 0.02877 | 348.14 | 0.000 | 62.43 |
| Sliding Velocity, m/s | 2 | 0.02337 | 0.02337 | 0.01168 | 141.36 | 0.000 | 25.35 |
| Sliding Distance, m | 2 | 0.00053 | 0.00053 | 0.00027 | 3.21 | 0.095 | 0.58 |
| Load, N*Sliding Velocity, m/s | 4 | 0.00295 | 0.00295 | 0.00074 | 8.93 | 0.005 | 3.20 |
| Load, N*Sliding Distance, m | 4 | 0.00098 | 0.00098 | 0.00025 | 2.96 | 0.089 | 1.06 |
| Sliding Velocity, m/s*Sliding Distance, m | 4 | 0.00613 | 0.00613 | 0.00153 | 18.56 | 0.000 | 6.66 |
| Error | 8 | 0.000661 | 0.000661 | 0.0000826 | | | 0.72 |
| Total | 26 | 0.092167 | | | | | 100.00 |

S = 0.00909100, R-Sq = 99.28%, R-Sq(adj) = 97.67%
[a] Degrees of freedom, [b] Sequential sums of squares, [c] Adjusted sums of squares, [d] Adjusted mean squares, [e] Probability

TABLE 4

Response table for SN ratio of coefficient of friction

| Level | Load, N | Sliding Velocity, m/s | Sliding distance, m |
|---|---|---|---|
| 1 | 22.74 | 12.33 | 17.53 |
| 2 | 14.04 | 14.70 | 15.81 |
| 3 | 11.03 | 20.78 | 14.47 |
| Delta | 11.71 | 8.45 | 3.07 |
| Rank | 1 | 2 | 3 |

### 3.2.2. Consequence of sliding velocity on specific wear rate and coefficient of friction

The sliding velocity has also put forth its effect over specific wear rate and coefficient of friction. The influence of sliding velocity on the specific wear rate is ranked 2 with the delta value of 5.98. Besides, the sliding velocity shows its significance on

value of 0.095 (Greater than 0.05). Likewise, the sliding distance is positioned at rank 3 for the coefficient of friction with the least delta value of 3.07 from the response table (TABLE 4). Though the analysis of variance (TABLE 5) shows significance to the parameter sliding distance, the contribution of the parameter is significantly less with the percentage of 2.71.

### 3.2.4. Model development and Validation of results

To estimate the tribological response specific wear rate and coefficient of friction, a mathematical model Eq. (1) and Eq. (2) is established with the help of general linear regression. The established model shows the regression coefficient of 98.71 for specific wear rate and 99.50 for the coefficient of friction. Using the established relation, the specific wear rate and coefficient of friction are calculated and equated with the experimental results,

TABLE 5

Analysis of variance of coefficient of friction

| Parameters | DF[a] | Seq SS[b] | Adj SS[c] | Adj MS[d] | F | P[e] | C% |
|---|---|---|---|---|---|---|---|
| Load, N | 2 | 0.12855 | 0.12855 | 0.06427 | 1475.97 | 0.000 | 65.84 |
| Sliding Velocity, m/s | 2 | 0.03857 | 0.03857 | 0.01929 | 442.89 | 0.000 | 19.76 |
| Sliding Distance, m | 2 | 0.00529 | 0.00529 | 0.00264 | 60.70 | 0.000 | 2.71 |
| Load, N*Sliding Velocity, m/s | 4 | 0.02222 | 0.02222 | 0.00556 | 127.57 | 0.000 | 11.38 |
| Load, N*Sliding Distance, m | 4 | 0.00003 | 0.00003 | 0.00001 | 0.18 | 0.942 | 0.02 |
| Sliding Velocity, m/s*Sliding Distance, m | 4 | 0.00022 | 0.00022 | 0.00006 | 1.29 | 0.351 | 0.11 |
| Error | 8 | 0.00035 | 0.00035 | 0.00004 | | | 0.18 |
| Total | 26 | 0.19524 | | | | | 100.00 |

S = 0.00659904, R-Sq = 99.82%, R-Sq(adj) = 99.42%
[a] Degrees of freedom, [b] Sequential sums of squares, [c] Adjusted sums of squares, [d] Adjusted mean squares, [e] Probability

TABLE 6

Validation of specific wear rate

| Exp. No | Load N | Sliding Velocity m/s | Sliding Distance m | Specific wear rate × 10⁻³ mm³/Nm | | Error % | Accu-racy % |
|---|---|---|---|---|---|---|---|
| | | | | Experiment | Predicted | | |
| 1 | 9.81 | 1 | 1000 | 0.1200 | 0.11368 | 5.27 | 94.73 |
| 2 | 9.81 | 1 | 2000 | 0.1412 | 0.13952 | 1.19 | 98.81 |
| 3 | 9.81 | 1 | 3000 | 0.1703 | 0.16536 | 2.90 | 97.10 |
| 4 | 9.81 | 1.5 | 3000 | 0.1257 | 0.12849 | 2.21 | 97.79 |
| 5 | 9.81 | 2 | 1000 | 0.0851 | 0.08477 | 0.39 | 99.61 |
| 6 | 9.81 | 2 | 1500 | 0.0848 | 0.08648 | 1.95 | 98.05 |
| 7 | 9.81 | 2 | 2000 | 0.0840 | 0.08820 | 5.00 | 95.00 |
| 8 | 9.81 | 2 | 3000 | 0.0823 | 0.09163 | 11.34 | 88.66 |
| 9 | 9.81 | 3 | 1000 | 0.0503 | 0.05586 | 11.05 | 88.95 |
| 10 | 9.81 | 3 | 2000 | 0.0400 | 0.03688 | 7.80 | 92.20 |
| 11 | 9.81 | 3 | 3000 | 0.0270 | 0.01790 | 33.70 | 66.30 |
| 12 | 14.72 | 3 | 3000 | 0.0502 | 0.04960 | 1.20 | 98.80 |
| 13 | 19.62 | 1 | 1000 | 0.1537 | 0.16334 | 6.27 | 93.73 |
| 14 | 19.62 | 1 | 2000 | 0.1836 | 0.18069 | 1.59 | 98.41 |
| 15 | 19.62 | 1 | 3000 | 0.1931 | 0.19803 | 2.56 | 97.44 |
| 16 | 19.62 | 1.5 | 3000 | 0.1693 | 0.16885 | 0.27 | 99.73 |
| 17 | 19.62 | 2 | 1000 | 0.1400 | 0.14979 | 6.99 | 93.01 |
| 18 | 19.62 | 2 | 2000 | 0.1535 | 0.14473 | 5.72 | 94.28 |
| 19 | 19.62 | 2 | 2500 | 0.1399 | 0.14220 | 1.64 | 98.36 |
| 20 | 19.62 | 2 | 3000 | 0.1386 | 0.13967 | 0.77 | 99.23 |
| 21 | 19.62 | 3 | 1000 | 0.1460 | 0.13623 | 6.69 | 93.31 |
| 22 | 19.62 | 3 | 2000 | 0.1108 | 0.10877 | 1.84 | 98.16 |
| 23 | 19.62 | 3 | 3000 | 0.0704 | 0.08130 | 15.48 | 84.52 |
| 24 | 24.53 | 3 | 3000 | 0.1136 | 0.11299 | 0.53 | 99.47 |
| 25 | 29.43 | 1 | 1000 | 0.2109 | 0.21300 | 1.00 | 99.00 |
| 26 | 29.43 | 1 | 2000 | 0.2309 | 0.22186 | 3.92 | 96.08 |
| 27 | 29.43 | 1 | 3000 | 0.2340 | 0.23071 | 1.41 | 98.59 |
| 28 | 29.43 | 1.5 | 3000 | 0.2114 | 0.20921 | 1.04 | 98.96 |
| 29 | 29.43 | 2 | 1000 | 0.2201 | 0.21481 | 2.40 | 97.60 |
| 30 | 29.43 | 2 | 2000 | 0.1994 | 0.20125 | 0.93 | 99.07 |
| 31 | 29.43 | 2 | 2500 | 0.1912 | 0.19448 | 1.71 | 98.29 |
| 32 | 29.43 | 2 | 3000 | 0.1765 | 0.18770 | 6.35 | 93.65 |
| 33 | 29.43 | 3 | 1000 | 0.2118 | 0.21661 | 2.27 | 97.73 |
| 34 | 29.43 | 3 | 2000 | 0.1795 | 0.18065 | 0.64 | 99.36 |
| 35 | 29.43 | 3 | 3000 | 0.1546 | 0.14469 | 6.41 | 93.59 |
| Average | | | | | | 4.64 | 95.36 |

TABLE 7

Validation of coefficient of friction

| Exp. No | Load N | Sliding Velocity m/s | Sliding Distance m | Coefficient of friction | | Error % | Accu-racy % |
|---|---|---|---|---|---|---|---|
| | | | | Experiment | Predicted | | |
| 1 | 9.81 | 1 | 1000 | 0.1805 | 0.1834 | 1.61 | 98.39 |
| 2 | 9.81 | 1 | 2000 | 0.2180 | 0.2033 | 6.75 | 93.25 |
| 3 | 9.81 | 1 | 3000 | 0.2155 | 0.2231 | 3.55 | 96.45 |
| 4 | 9.81 | 1.5 | 3000 | 0.1791 | 0.1774 | 0.95 | 99.05 |
| 5 | 9.81 | 2 | 1000 | 0.0912 | 0.0966 | 5.97 | 94.03 |
| 6 | 9.81 | 2 | 1500 | 0.1079 | 0.1054 | 2.32 | 97.68 |
| 7 | 9.81 | 2 | 2000 | 0.1131 | 0.1142 | 0.95 | 99.05 |
| 8 | 9.81 | 2 | 3000 | 0.1248 | 0.1317 | 5.49 | 94.51 |
| 9 | 9.81 | 3 | 1000 | 0.0071 | 0.0099 | 38.30 | 61.70 |
| 10 | 9.81 | 3 | 2000 | 0.0169 | 0.0250 | 48.05 | 51.95 |
| 11 | 9.81 | 3 | 3000 | 0.0446 | 0.0402 | 9.95 | 90.05 |
| 12 | 14.72 | 3 | 3000 | 0.1049 | 0.1036 | 1.28 | 98.72 |
| 13 | 19.62 | 1 | 1000 | 0.2216 | 0.2255 | 1.77 | 98.23 |
| 14 | 19.62 | 1 | 2000 | 0.2489 | 0.2449 | 1.61 | 98.39 |
| 15 | 19.62 | 1 | 3000 | 0.2647 | 0.2643 | 0.16 | 99.84 |
| 16 | 19.62 | 1.5 | 3000 | 0.2385 | 0.2399 | 0.60 | 99.40 |
| 17 | 19.62 | 2 | 1000 | 0.1835 | 0.1816 | 1.04 | 98.96 |
| 18 | 19.62 | 2 | 2000 | 0.2074 | 0.1986 | 4.24 | 95.76 |
| 19 | 19.62 | 2 | 2500 | 0.2096 | 0.2071 | 1.19 | 98.81 |
| 20 | 19.62 | 2 | 3000 | 0.2140 | 0.2156 | 0.75 | 99.25 |
| 21 | 19.62 | 3 | 1000 | 0.1462 | 0.1377 | 5.84 | 94.16 |
| 22 | 19.62 | 3 | 2000 | 0.1598 | 0.1523 | 4.69 | 95.31 |
| 23 | 19.62 | 3 | 3000 | 0.1726 | 0.1670 | 3.27 | 96.73 |
| 24 | 24.53 | 3 | 3000 | 0.2326 | 0.2304 | 0.96 | 99.04 |
| 25 | 29.43 | 1 | 1000 | 0.2645 | 0.2676 | 1.19 | 98.81 |
| 26 | 29.43 | 1 | 2000 | 0.2801 | 0.2865 | 2.29 | 97.71 |
| 27 | 29.43 | 1 | 3000 | 0.3098 | 0.3054 | 1.42 | 98.58 |
| 28 | 29.43 | 1.5 | 3000 | 0.3001 | 0.3025 | 0.79 | 99.21 |
| 29 | 29.43 | 2 | 1000 | 0.2706 | 0.2665 | 1.50 | 98.50 |
| 30 | 29.43 | 2 | 2000 | 0.2896 | 0.2831 | 2.26 | 97.74 |
| 31 | 29.43 | 2 | 2500 | 0.2939 | 0.2913 | 0.88 | 99.12 |
| 32 | 29.43 | 2 | 3000 | 0.2942 | 0.2996 | 1.83 | 98.17 |
| 33 | 29.43 | 3 | 1000 | 0.2582 | 0.2655 | 2.81 | 97.19 |
| 34 | 29.43 | 3 | 2000 | 0.2755 | 0.2796 | 1.49 | 98.51 |
| 35 | 29.43 | 3 | 3000 | 0.2894 | 0.2938 | 1.51 | 98.49 |
| Average | | | | | | 4.84 | 95.16 |

as shown in TABLE 6 and 7. Besides, the tribological responses beyond the data source is predicted by varying the parameters in a radom condition and it is shown in TABLE 6 and 7. Further, the experimentation was done for the parameter combination beyond the data source and the same is compared with the predicted results. The comparison results displayed the average error percentage of 4.64 for specific wear rate and 4.84 for coefficient of friction. Figure 4a and 4b displays the comparison of estimated and experimental tribological responses specific wear rate and coefficient of friction, respectively. The estimated tribological responses show the least error percentage with closer estimated results to the experimental value. Thus, the established model shows enough conformity with the tribological responses.

$$\text{Specific wear rate, mm}^3/\text{Nm} = 0.0515481 +$$
$$0.00436233\ A - 0.0218611\ B + 5.67389e -$$
$$005\ C + 0.00156558\ A * B - 8.65613e -$$
$$007\ A * C - 2.24083e - 005\ B * C \qquad (1)$$

$$\text{Coefficient of friction} = 0.248182 - 2.33379e -$$
$$005\ A - 0.127245\ B + 2.27255e - 005\ C +$$
$$0.00436679\ A * B - 5.06201e -$$
$$008\ A * C - 2.36175e - 006\ B * C \qquad (2)$$

### 3.3. Wear mechanisms

The morphological analysis on the worn surface of additive manufactured titanium alloy shown in Figure 5 exhibits the governing wear mechanisms. The worn surface morphology of the additive manufactured titanium alloy with the highest wear rate, and the lowest wear rate is shown in Figure 5a and 5b, respectively. Figure 5a displays the existence of grooves, ploughs, and craters, which shows the existence of abrasion and delamination mechanism [19,20,31]. Also, the existence of more number of craters shows the dominance of delamination mechanism, which ended up in the higher material wear. The wear debris
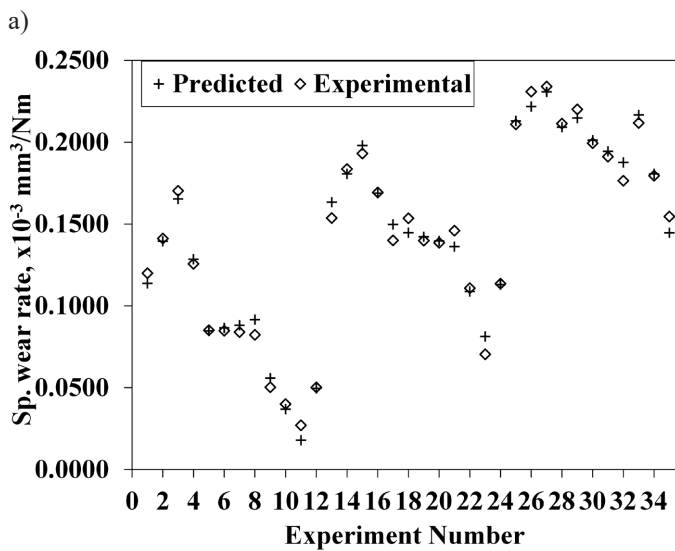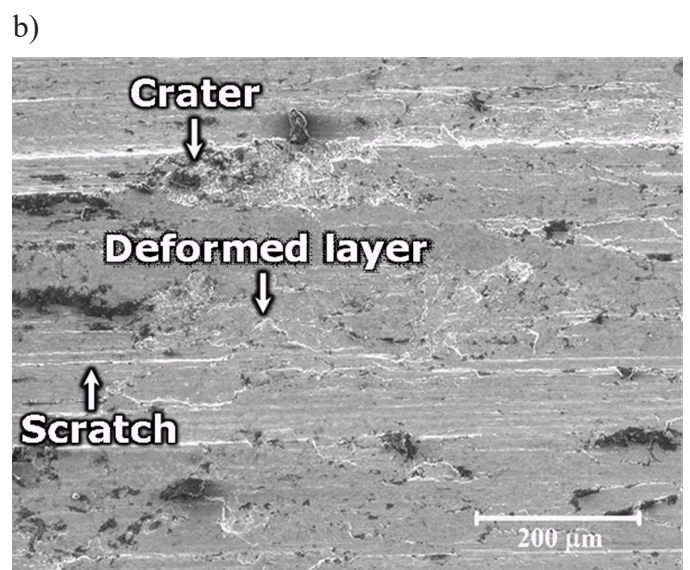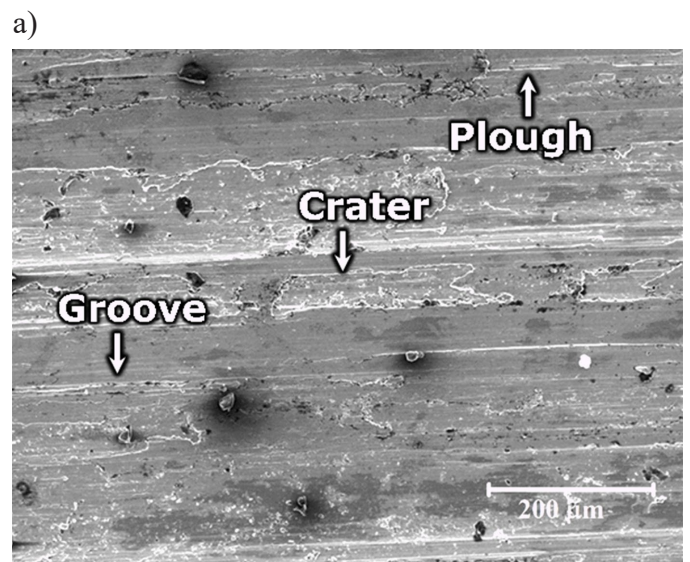
a)



b)



Fig. 4. Comparison of estimated results with experimental results: (a) specific wear rate; (b) coefficient of friction

a)



b)



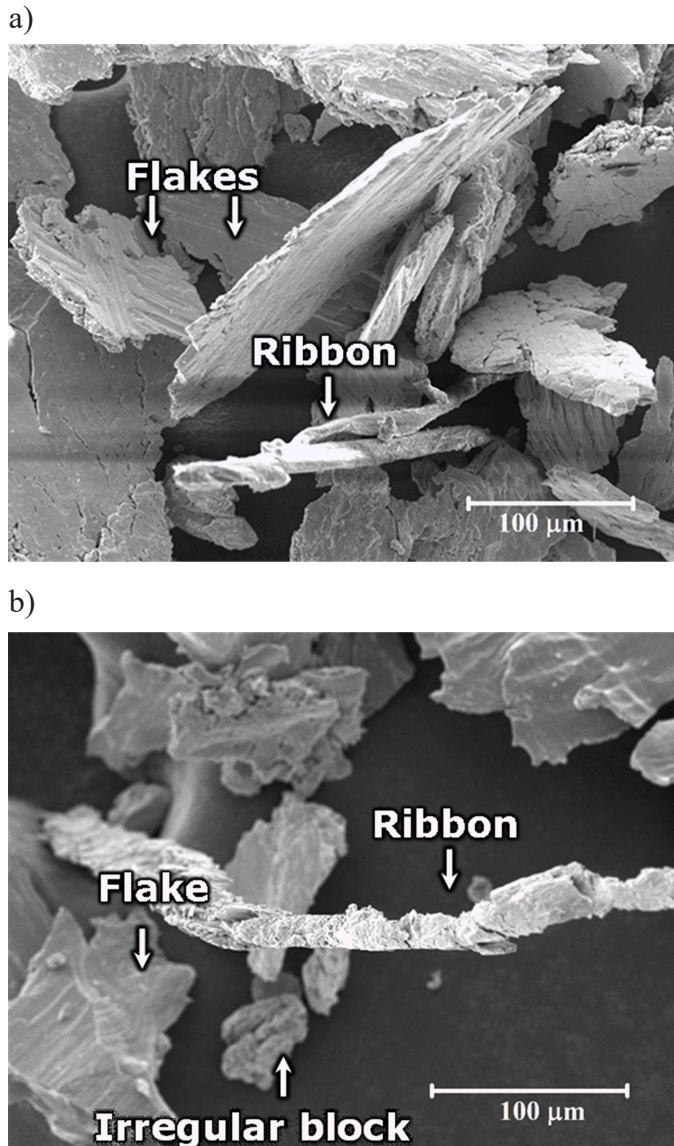Fig. 5. Worn surface analysis at: (a) highest wear; (b) lowest wear

a)



b)



Fig. 6. Debris analysis at: (a) highest wear; (b) lowest wear

(Figure 6a) pertains to the highest wear condition displays the ribbon strips and flakes, which confirms the abrasion and delamination mechanisms. Figure 5b displays the existence of scratches, craters and deformed layers which shows the existence of abrasion, delamination and adhesion mechanisms [19,20,31]. The wear debris (Figure 6b) pertains to the lowest wear condition displays the ribbon strip, flakes and irregular block which confirms the abrasion and delamination mechanisms.

### 4. Conclusions

The titanium alloy (Ti-6Al-4V) was produced through the additive manufacturing technique with a novel prepositioning method. The metallurgical analysis performed on the additive manufactured titanium alloy displays the α phase. The tribology of the additive manufactured titanium alloy under dry sliding condition was analysed using Taguchi technique. The required objective of the minimum tribological responses can be attained

with the optimal solution; for specific wear rate: load – 9.81 N, sliding velocity – 3 m/s, sliding distance – 3000 m and for the coefficient of friction: 9.81 N, sliding velocity – 3 m/s, sliding distance – 1000 m. The tribological responses calculated with the established model show 94% of accuracy. The morphological analysis on the worn surface and debris reveals the existence of abrasion, delamination and adhesion mechanisms.

## REFERENCES

[1] A. Eakambaram, M.A. Xavior, Arch. Metall. Mater. **64**, 1541-1548 (2019). DOI: https://doi.org/10.24425/amm.2019.130124
[2] D.A. Angel, T. Miko, M. Benke, Z. Gacsi, Arch. Metall. Mater. **65**, 515-519 (2020). DOI: https://doi.org/10.24425/amm.2020.132788
[3] A. Woźniak, O. Bialas, M. Adamiak, Arch. Metall. Mater. **65**, 735-741 (2020). DOI: https://doi.org/10.24425/amm.2020.132813
[4] M. Elguerri, Tec. Ital. J. Eng. Sci. **64**, 216-224 (2020). DOI: https://doi.org/10.18280/ti-ijes.642-414
[5] S. Dwivedi, S. Chauhan, Tec. Ital. J. Eng. Sci. **64**, 259-264 (2020). DOI: https://doi.org/10.18280/ti-ijes.642-420
[6] ISO/ASTM. 52900:2015, ASTM Int. 1-9 (2015). DOI: https://doi.org/10.1520/ISOASTM52900-15
[7] S.M. Kelly, S.L. Kampe, Metall. Mater. Trans. A Phys. Metall. Mater. Sci. **35** A, 1869-1879 (2004). DOI: https://doi.org/10.1007/s11661-004-0095-7
[8] L. Thijs, F. Verhaeghe, T. Craeghs, J. Van Humbeeck, J.P. Kruth, Acta Mater. **58**, 3303-3312 (2010). DOI: https://doi.org/10.1016/j.actamat.2010.02.004
[9] F. Verhaeghe, T. Craeghs, J. Heulens, L. Pandelaers, Acta Mater. **57**, 6006-6012 (2009). DOI: https://doi.org/10.1016/j.actamat.2009.08.027
[10] D. Bourell, J.P. Kruth, M. Leu, G. Levy, D. Rosen, A.M. Beese, A. Clare, CIRP Ann. – Manuf. Technol. **66**, 659-681 (2017). DOI: https://doi.org/10.1016/j.cirp.2017.05.009
[11] A. Manjunath, V. Anandakrishnan, S. Ramachandra, K. Parthiban, Mater. Today Proc. **21**, 766-772 (2019). DOI: https://doi.org/10.1016/j.matpr.2019.06.727
[12] J. Fuchs, C. Schneider, N. Enzinger, Weld. World. **62**, 267-275 (2018). DOI: https://doi.org/10.1007/s40194-017-0537-7
[13] Q. Wu, J. Lu, C. Liu, X. Shi, Q. Ma, S. Tang, H. Fan, S. Ma, Mater. Manuf. Process. **32**, 1881-1886 (2017). DOI: https://doi.org/10.1080/10426914.2017.1364860.
[14] M. Weglowski, Trends Civ. Eng. Its Archit. **1**, 25-26 (2018). DOI: https://doi.org/10.32474/tceia.2018.01.000106
[15] P. Wanjara, K. Watanabe, C. De Formanoir, Q. Yang, C. Bescond, S. Godet, M. Brochu, K. Nezaki, J. Gholipour, P. Patnaik, Adv. Mater. Sci. Eng. (2019). DOI: https://doi.org/10.1155/2019/3979471
[16] M.D. Sharma, R. Sehgal, Ind. Lubr. Tribol. **66**, 174-183 (2014). DOI: https://doi.org/10.1108/ILT-10-2011-0079
[17] D. Kumar, K.B. Deepak, S.M. Muzakkir, M.F. Wani, K.P. Lijesh, Tribol. – Mater. Surfaces Interfaces. **12**, 137-143 (2018). DOI: https://doi.org/10.1080/17515831.2018.1482676
[18] X.X. Li, Y. Zhou, X.L. Ji, Y.X. Li, S.Q. Wang, Tribol. Int. **91**, 228-234 (2015). doi:10.1016/j.triboint.2015.02.009

454

[19] A. Molinari, G. Straffelini, B. Tesi, T. Bacci, Wear. **208**, 105-112 (1997). DOI: https://doi.org/10.1016/S0043-1648(96)07454-6

[20] Y. Zhu, X. Chen, J. Zou, H. Yang, Wear. **368-369**, 485-495 (2016). DOI: https://doi.org/10.1016/j.wear.2016.09.020

[21] M.O. Alam, A.S.M.A. Haseeb, Tribol. Int. **35**, 357-362 (2002). DOI: https://doi.org/10.1016/S0301-679X(02)00015-4

[22] Q. An, L.J. Huang, Y. Bao, R. Zhang, S. Jiang, L. Geng, M. Xiao, Tribol. Int. **121**, 252-259 (2018). DOI: https://doi.org/10.1016/j.triboint.2018.01.053

[23] M. Dutt Sharma, R. Sehgal, Tribol. Online. **7**, 87-95 (2012). DOI: https://doi.org/10.2474/trol.7.87.

[24] Q. Ming, Z. Yong-zhen, Y. Jian-heng, Z. Jun, Mater. Sci. Eng. A. **434**, 71-75 (2006). DOI: https://doi.org/10.1016/j.msea.2006.07.043

[25] G.D. Revankar, R. Shetty, S.S. Rao, V.N. Gaitonde, J. Mater. Res. Technol. **6**, 13-32 (2017). DOI: https://doi.org/10.1016/j.jmrt.2016.03.007

[26] S. Sathish, V. Anandakrishnan, G. Manoj, Mater. Today Proc. **21**, 492-496 (2020). DOI: https://doi.org/10.1016/j.matpr.2019.06.643

[27] S. Sathish, V. Anandakrishnan, G. Manoj, Ind. Lubr. Tribol. **72**, 503-508 (2019). DOI: https://doi.org/10.1108/ILT-08-2019-0326

[28] S. Sathish, V. Anandakrishnan, S. Sankaranarayanan, M. Gupta, J. Tribol. **23**, 76-89 (2019).

[29] J. Matthew J. Donachie, Titanium – A Techinacal Guide, (2000). DOI: https://doi.org/10.5772/1844.

[30] C. Saravanan, V. Subramanian, K. Anandakrishnan, S. Sathish, Ind. Lubr. Tribol. **70**, 1066-1071 (2018). DOI: https://doi.org/10.1108/ILT-10-2017-0312

[31] M. Ananda Jothi, S. Ramanathan, Mater. Sci. Forum. **830-831**, 333-336 (2015). DOI: https://doi.org/10.4028/www.scientific.net/MSF.830-831.333